
EEG-fMRI Source Localization: Final Report

Wusheng Liang, Eli Bulger, Jingyi Wu
Department of Biomedical Engineering
Carnegie Mellon University
Pittsburgh, PA 15213

1 Introduction

One of the most important problems in neurophysiology is to identify the exact location inside the brain that corresponds to measured neural activity. One way to do this is referred to as source localization, which is important for clinical applications, such as the study of evoked-related-potentials, localized epilepsy, attention deficit/hyperactivity disorder and more.[1].

Electroencephalography (EEG) is commonly used to non-invasively measure the electrical activity of the brain. It detects the voltages from the synchronized activated neurons in the cerebral cortex. However, the detected signal on the scalp cannot be used to accurately estimate the neurons which generated the measured potentials, which causes difficulties in trying to interpret the brain regions where neuronal activity originates [2]. On the other hand, fMRI, which is commonly used to measure the blood oxygen level dependent (BOLD) signal from neural activity, has high spatial resolution. Thus, incorporating fMRI information into standard EEG source localization can provide a better result [3]. In this report, we will discuss source localization techniques and results of using EEG only, and EEG+fMRI.

2 Related Work

From the literature, source modelling for neuron activity is usually divided into the forward and the inverse problem [4]. The forward problem tries to find the relationship describing how the scalp potentials are affected by the hypothetical dipoles (neural sources), and the inverse problem tries to use the forward model to estimate the sources from scalp potential measurements [5]. In addition, assumptions about the dipole distribution can be made, leading to two main source localization methods: (1) Parametric method, which assumes that only a small number of dipoles generating the scalp potentials and uses non-linear optimizations to solve the best dipole location and orientation parameters [1,5]. (2) Non-parametric method, which assumes many dipoles are distributed across the cortical surface with fixed locations and fixed orientations [6].

Under some specific setups, such as high density EEG systems and precise head anatomy, Michel et al. demonstrated that EEG can be used to properly localize the source [2]. Other work has incorporated fMRI data as a prior for EEG to constrain source localization to highly active regions as seen by fMRI [3]. In our current work, we performed source-localization using the EEG data, and will be following a method similar to [3] to incorporate fMRI data. Since we don't have ground truth source locations, as some simulation-generated datasets may have, we attempt to observe the different source locations based on event related neuron activities.

3 Methods

3.1 Dataset

The datasets were collected by Winko An and Alexander Pei at Boston University. The EEG data was collected from 30 participants between ages of 19 and 44 (14 females, 16 males), and the MRI data was collected from 19 participants between ages of 19 and 30 (8 females, 11 males), with no self-reported hearing loss or history of neurological disorders in both datasets. For both datasets, the participants were required to do the same auditory attention task during the recording, and they were required to use either spatial attention (attend to a specific spatial direction) or talker attention (attend to a specific talker) to identify a target syllable or just relax / listen to the stimuli passively. The experimental schematic is shown in Figure 1.

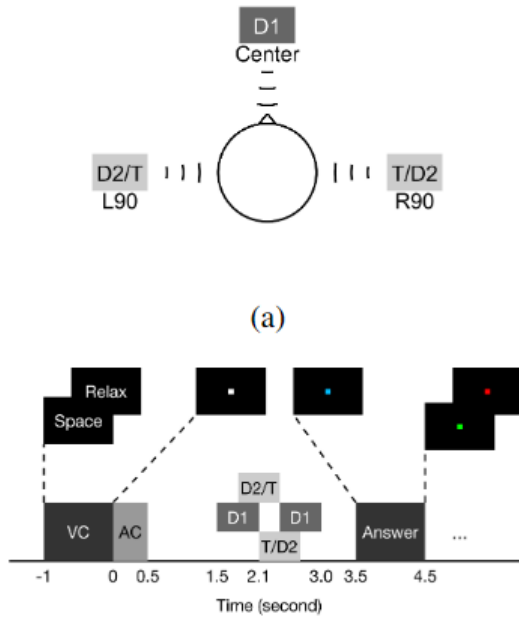


Figure 1: Schematic of the task design

The EEG data structure is a biosemi .bdf data object with metadata and 64 channels of EEG data, with an epoch for each trial. The data is split in 747 trials from 21 different experimental conditions. The fMRI dataset is composed of data from the same experiment, and is designed to look at regional activation from different task types (i.e. attention towards a spatial direction vs. attention towards a talker). The data structure extracted from fMRI is a 163842 x 1 vector, with each value corresponding to a brain activation level representing regions active during spatial attention. Each index corresponds to a spatial location in a standard brain surface space.

3.2 EEG Only: Forward Model

We implemented a baseline model for EEG source localization with Python-MNE. The uninformed EEG model consists of the development of a forward model, an inverse model, and the localized sources from our EEG dataset ($n=1$) using the inverse model. The baseline model mainly contains 3 steps, first is to prepare the subject-specific anatomical surfaces (using Freesurfer software), which is needed for computing the forward model, second is to compute the forward model, and finally, the inverse model.

The forward model is also known as a gain or leadfield matrix, and it represents how neural source locations affect the scalp potentials that EEG electrodes record. The first step in calculating the forward model was to generate a boundary element model (BEM) surface that contains information on the head anatomy, including the skin, scalp, and brain. This BEM surface (see Figure 2) takes

into account the subject-specific anatomical structure (T1w scans) as given by reconstruction from MRI data. The next step was specifying the EEG electrode distribution (a 64-channel montage), and registering (projecting) that distribution to the subject-specific scalp surface (see Figure 3). Afterwards, we generated a source space composed on possible neural generator locations on the brain's surface (see Figure 3). Using the BEM model, the source space, and the registered electrode locations, a forward model containing a matrix of size $\text{num_of_channels} \times \text{num_neural_sources}$ was created, describing how each neural source contributes to EEG electrode recordings. Results from the forward model are showed in Figure 2-3.

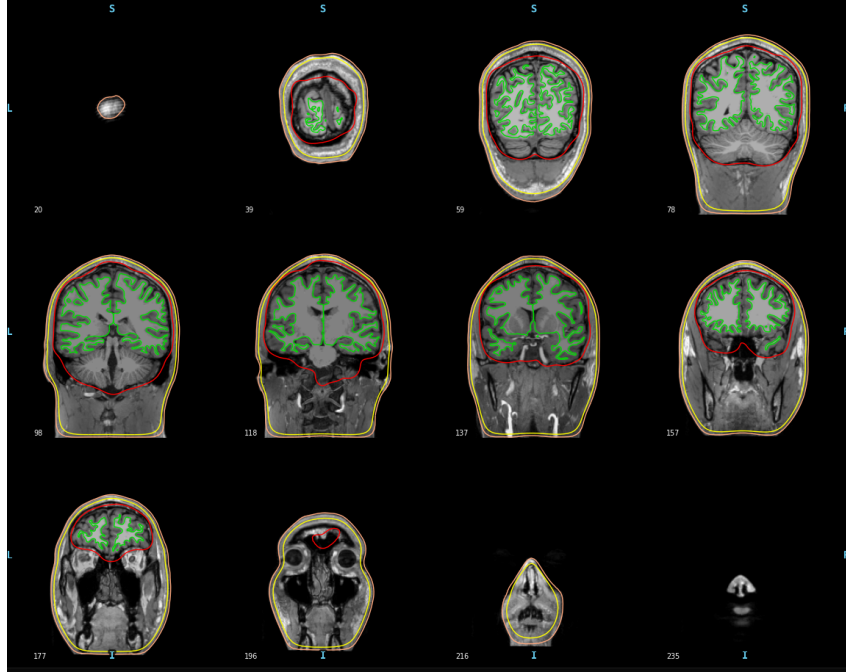


Figure 2: BEM surface at different cross-sections outlining the estimated brain surface in red, the grey matter in green, and the scalp and skin surfaces in orange and yellow.

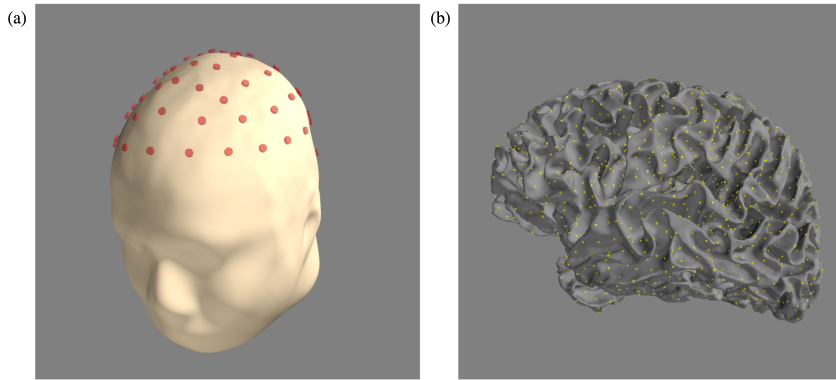


Figure 3: (a) The subject-specific scalp anatomy with 64 projected EEG electrode positions (red). (b) The generated neural sources (yellow) on the subject-specific brain surface (grey).

3.3 EEG Only: Inverse Model

We used the MNE package with Python for the inverse computation. With Python-MNE, the process of computing the inverse solution with minimum-norm current estimates is to: 1) baseline correct the data by subtracting the mean signal of the baseline period of the trials (0.5s time period before onset of

the stimuli of interest), 2) compute the noise covariance matrix with 0.5s time period before the onset of the stimuli of interest, which is needed for computing the inverse operator, 3) load the forward model and compute inverse operator M with evoked data, forward model and noise covariance matrix, here M is a $Q \times N$ matrix, Q stands for the number of sources strength on the cortical, N is the number of electrodes, 4) solve the current amplitude at time t with the inverse operator with $\hat{j}(t) = Mx(t)$. The result is a *number_of_sources × time_points* matrix, containing the solved source time course.

The following regularized least squares regression equation is typically used as a basis to solve the inverse problem:

$$J = WK^T(KWK^T + \lambda^2 C)^{-1}M \quad (1)$$

where J is the source generator activity, W is a source covariance matrix, K is the calculated lead field/source model, C is typically the identity matrix, λ is a regularization parameter, and M contains the measured electric potentials [1, 2].

Several different methods are supported for source localization in the MNE package, including minimum norm estimation (MNE), dynamic statistical parametric mapping (dSPM), and standardized low-resolution electromagnetic tomography (sLORETA). The difference between them is the way they normalize the current density map, MNE doesn't normalize the current density map, while dSPM and sLORETA normalized the current density map with the variance estimation of either the noise or the theoretical data at each location in the current density map [9].

Another parameter that would have a significant affect on the source localization result is the regularization parameter λ . A previous study has pointed out that with their simulated data, a bigger regularization parameter λ , the result will be more smoothed, the sensitivity in coherence analysis will drop, and a smaller regularization parameter could lead to a better coherence detection, they also indicated that a regularization parameter that improves the detection of oscillatory source power may impair the ability to reconstruct the spectral connectivity, so there's also no single best λ option[10].

In addition, we constructed the forward and inverse models using EEGLAB, which is a widely used Matlab toolbox for EEG data processing. However, since python MNE is more robust in selecting methods for source localization, tuning parameters, and incorporating the MRI data. We stopped using EEGLAB for this project. Additional information about the EEGLAB implementation is included in Appendix A.

3.4 EEG Source Localization with fMRI Prior

Next, we incorporated fMRI data as a prior to constrain EEG source localization. To do this, we first defined highly activated regions in fMRI data as the top 50% activation of the spatially activated regions (red regions in Figure 5a). We then converted this to a boolean array in fsaverage space, resulting in a binary 163842 x 1 vector, where non-zero values corresponded to highly activated regions. The vertices in the standard space nearest to those in the subject specific space (matching the forward model) were then found using a nearest-neighbours approach, as computed by Python-MNE. This resulted in two 2562 x 1 source space vectors (one for each hemisphere). These hemispheres were combined to form a 5124 x 1 vector for the whole brain. The binary format was converted according to the following equation:

$$F'_i = \frac{F_i + 0.5}{2} \quad (2)$$

where F is the binary fMRI mask, and F' is a "soft" mask holding values of 0.75 and 0.25. We incorporated fMRI as a prior by a simple dot product between the F' and the trace of the source covariance matrix in the least-squares regularization scheme. By doing this, we essentially weighted the regions activated in fMRI greater than those not activated in fMRI, without completely removing activity that did not agree between EEG and fMRI. While we initially planned to edit the off-diagonal terms of the source covariance term in order to reduce spatial smoothing of the solution, we chose to directly edit the diagonal terms due to ease of implementation and easy interpretability.

4 Results

Results for source localization with only EEG data are shown in Figure 4, the upper parts of the plots are the back views of the 3D brain, with source activation plot on it, the bottom parts of the plots are the source energy over time on left (blue line) and right (orange line) hemisphere.

Comparing the MNE, dSPM, and sLORETA methods with regularization parameter λ equal to 0.1 (Figure 4 a,b,c), we could tell that the results for the 3 methods are quite different, but dSPM and sLORETA are more similar since they both normalized the current density map while MNE does not. Methods that normalizes current density maps are normally preferred over those doesn't, and comparing the methods with normalized current density maps, dSPM could give higher values in deeper areas, while sLORETA can produce smoother maps regardless of the depth of the sources [9], there's no single best methods, each experiment could select the specific method best fits their goals.

Comparing the results of EEG-only source localization with different regularization parameter λ (Figure 4 d,e,f), the estimated source have similar trends, but the source energy is on a smaller scale with bigger λ , and the peak energy is the most condensed with the medium regularization parameter we tested with the dSPM method and our specific data.

Results for fMRI informed EEG source localization are shown in Figure 5.

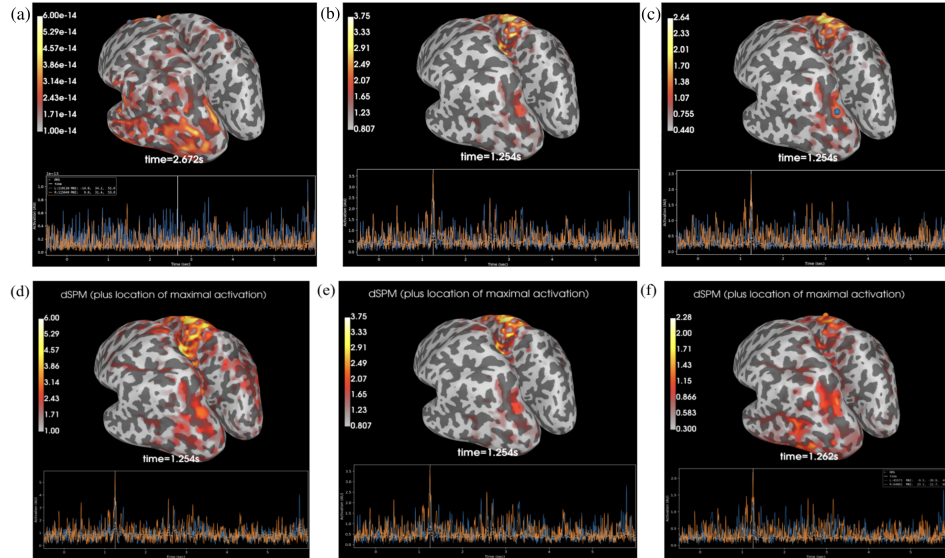


Figure 4: EEG-only Source Localization Results (a) MNE, $\lambda=0.1$ (b) dSPM, $\lambda=0.1$ (c) sLORETA, $\lambda=0.1$ (d) dSPM, $\lambda=0.001$, (e) dSPM, $\lambda=0.1$, (f) dSPM, $\lambda=1$

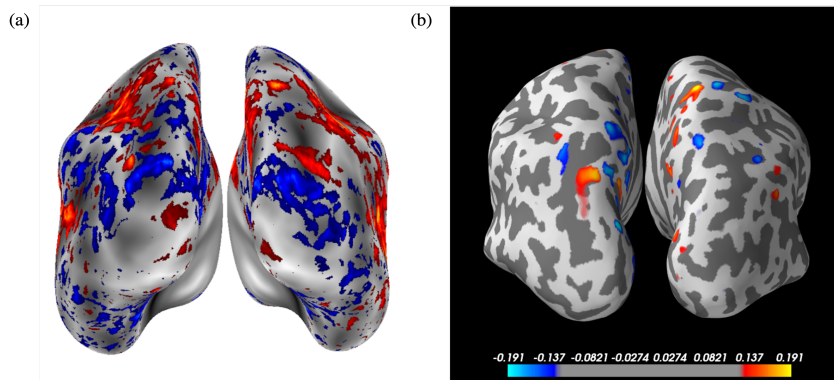


Figure 5: (a) fMRI prior before processing. (b) EEG+fMRI localization.

5 Discussion

Since ground truth source locations of the neuron activities are not available in our dataset, we investigated different EEG source localization inverse algorithms in MNE (dSPM, LORETA, etc.). Results are shown in Figure 4.

As an evaluation metric for implementing fMRI as prior data, we compared the solutions using EEG alone and both fMRI and EEG. We did this by determining which method has greater spatial resolution and results that align with hypothesized performance. While we initially planned to look at alpha power localization in parietal lobe as a measure of performance, we were unable to use this as a metric due to the inherent noise in the data. Instead, we found that the fMRI-informed EEG source localization has higher spatial resolution that more closely matched that of the fMRI prior, marking a decrease in source localization variance and increase in accuracy. Figure 6 shows the comparison between EEG source localization and fMRI informed EEG source localization results.

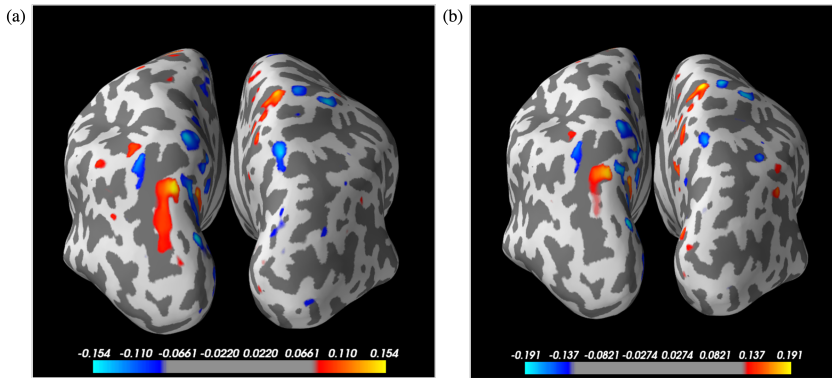


Figure 6: (a) EEG only. (b) EEG+fMRI.

References

- [1] Muñoz-Gutiérrez, P. A., Giraldo, E., Bueno-López, M., amp; Molinas, M. (2018). Localization of active brain sources from EEG signals using empirical mode decomposition: A comparative study. *Frontiers in Integrative Neuroscience*, 12. <https://doi.org/10.3389/fnint.2018.00055>
- [2] C.M. Michel, D. Brunet, EEG Source Imaging: A Practical Review of the Analysis Steps, *Front. Neurol.* 10 (2019) 325. <https://doi.org/10.3389/fneur.2019.00325>.
- [3] B.R. Cottreau, J.M. Ales, A.M. Norcia, How to use fMRI functional localizers to improve EEG/MEG source estimation, *J. Neurosci. Methods*. 250 (2015) 64–73. <https://doi.org/10.1016/j.jneumeth.2014.07.015>.
- [4] S. Asadzadeh, T. Yousefi Rezaei, S. Beheshti, A. Delpak, S. Meshgini, A systematic review of EEG source localization techniques and their applications on diagnosis of brain abnormalities, *J. Neurosci. Methods*. 339 (2020). <https://doi.org/10.1016/j.jneumeth.2020.108740>.
- [5] R. Grech, T. Cassar, J. Muscat, K.P. Camilleri, S.G. Fabri, M. Zervakis, P. Xanthopoulos, V. Sakkalis, B. Vanrumste, Review on solving the inverse problem in EEG source analysis, *J. Neuroeng. Rehabil.* 5 (2008) 1–33. <https://doi.org/10.1186/1743-0003-5-25>.
- [6] M. Luessi, S.D. Babacan, R. Molina, J.R. Booth, A.K. Katsaggelos, Bayesian symmetrical EEG/fMRI fusion with spatially adaptive priors, *Neuroimage*. 55 (2011) 113–132. <https://doi.org/10.1016/j.neuroimage.2010.11.037>.
- [7] C.M. Michel, B. He, EEG source localization, 1st ed., Elsevier B.V., 2019. <https://doi.org/10.1016/B978-0-444-64032-1.00006-0>.
- [8] R.J. Huster, S. Debener, T. Eichele, C.S. Herrmann, Methods for simultaneous EEG-fMRI: An introductory review, *J. Neurosci.* 32 (2012) 6053–6060. <https://doi.org/10.1523/JNEUROSCI.0447-12.2012>.
- [9] Hauk, Olaf, Daniel G. Wakeman, and Richard Henson. "Comparison of noise-normalized minimum norm estimates for MEG analysis using multiple resolution metrics." *Neuroimage* 54.3 (2011): 1966-1974.
- [10] Hincapié, Ana-Sofía, et al. "MEG connectivity and power detections with minimum norm estimates require different regularization parameters." *Computational intelligence and neuroscience* 2016 (2016).

Appendix A: EEGLAB

EEGLAB is a widely used Matlab toolbox for continuous and event-related EEG data processing. We originally planned to use it to learn the basic steps of the EEG source localization. To perform the localization, EEGLAB makes the assumption that the summed projections of the brain current dipoles to the scalp is very close to the observed scalp distribution. By choosing an appropriate head model and computing the dipole-to-scalp projection, we first acquired a forward from EEGLAB. Then, in the inverse problem, EEGLAB computes the best fit the active dipole (ICA component map) to the scalp map, and thus realizing the EEG source localization. Figure 7 (a) demonstrate a co-registered boundary element head model. Figure 7 (b) shows example extracted ICA components (with dipole projections). Figure 7 (c) shows the 3-D source localization results of the first three ICA components.

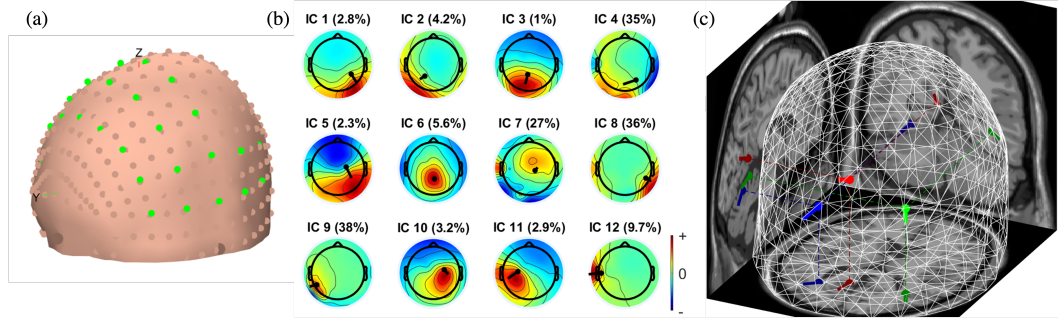


Figure 7: (a) Co-registered boundary element head model. (b) Extracted ICA components (with dipole projections). (c) 3-D source localization